

3DSwapping: Texture Swapping For 3D Object From Single Reference Image

Xiao Cao¹ Beibei Lin¹ Bo Wang²
Zhiyong Huang¹ Robby T. Tan¹

¹National University of Singapore ²University of Mississippi

{xiaocao, beibei.lin}@u.nus.edu, {dcshuang, robbey.tan}@nus.edu.sg, hawk.rsrch@gmail.com



Figure 1. Comparison of 2D and 3D methods for swapping texture from reference images onto target 3D scenes. Prompts are “moss covered table” and “pink plastic bear”. 2D methods Plug-n-Play [28] suffers from view inconsistency problem; 3D text-driven editing methods IGS2GS [29] and GaussCtrl [34] struggle to preserve texture characteristics. Ours faithfully swap texture, material appearance, and color.

Abstract

3D texture swapping allows for the customization of 3D object textures, enabling efficient and versatile visual transformations in 3D editing. While no dedicated method exists, adapted 2D editing and text-driven 3D editing approaches can serve this purpose. However, 2D editing requires frame-by-frame manipulation, causing inconsistencies across views, while text-driven 3D editing struggles to preserve texture characteristics from reference images. To tackle these challenges, we introduce 3DSwapping, a 3D texture swapping method that integrates: 1) progressive generation, 2) view-consistency gradient guidance, and 3) prompt-tuned gradient guidance. To ensure view consistency, our progressive generation process starts by editing a single reference image and gradually propagates the edits to adjacent views. Our view-consistency gradient guidance further reinforces consistency by conditioning the generation model on feature differences between consistent and

inconsistent outputs. To preserve texture characteristics, we introduce prompt-tuning-based gradient guidance, which learns a token that precisely captures the difference between the reference image and the 3D object. This token then guides the editing process, ensuring more consistent texture preservation across views. Overall, 3DSwapping integrates these novel strategies to achieve higher-fidelity texture transfer while preserving structural coherence across multiple viewpoints. Extensive qualitative and quantitative evaluations confirm that our three novel components enable convincing and effective 2D texture swapping for 3D objects. Code will be available upon acceptance.

1. Introduction

3D object texture swapping is an important and underdeveloped functionality in the 3D editing field. The ability to swap texture from a single image to a 3D object faith-

fully enables efficient and versatile 3D editing and can contribute to many 3D-related fields such as virtual reality, CG movies, and 3D games by saving costly texture-making processes [2, 25]. Although numerous methods for 2D texture swapping and 3D editing have been proposed, the task of applying textures from a single 2D image onto a 3D object in a visually convincing manner remains challenging. This difficulty comes primarily from issues with maintaining view consistency and preserving texture characteristics from a given input 2D image in swapping process.

2D swapping methods [10, 20, 26, 28, 37, 40, 40] can achieve swapping ability by finetuning stable diffusion (e.g., dreambooth [24], textural inversion [9]) and then edit images rendered from 3D object independently for constructing 3D finetuning dataset. After the aforementioned editing process, directly finetuning 3D object based on the obtained training set can give us the edited object, which exhibits view variations and significant identity loss due to a lack of view consistency and identity preservation constraints, as shown in Figure 1. **3D editing** methods [6, 7, 13, 18, 29, 32, 34, 41] (i.e., text-driven editing methods), can achieve swapping functionality by giving a prompt that specifically describes features of a reference image by the visual language model or human annotation. Nonetheless, text descriptions are coarse-grained. They lead to intermediate features that align in high-level semantics but diverge in fine-grained details, causing loss of identity and view inconsistency problems.

Motivated by the above problems, we propose a novel pipeline *3DSwapping* that swaps texture from a single reference 2D image to a 3D object represented by 3D Gaussian splatting. Specifically, our *3DSwapping* includes three main components: 1) progressive generation process, 2) view-consistency gradient guidance and 3) prompt-tuning based gradient guidance. Components 1 and 2 are designed to address the view inconsistency problem, while component 3 is to retain texture characteristics.

In the progressive generation process, we generate candidate images using a depth-conditioned model [38] on the unedited view’s depth and text prompt, then select the highest-quality image that best matches the prompt’s desired attributes. Next, we mask the background in both unedited training and reference images, and convert them to latent space for partial diffusion (Sec.3.1). Starting from the reference view, the process propagates to adjacent views using sparse cross-attention on previously edited images, ensuring maximum overlap between reference images to maintain view consistency.

To further improve diffusion’s view consistency awareness in 3D editing tasks, we propose view-consistency gradient guidance. The key idea is to enhance the view-consistency feature, thereby improving the diffusion model’s awareness of view consistency. We first initialize

two diffusion modules: one generates images while also conditions on the reference views, and the other generates images based on text prompt. We treat the difference of two diffusion’s intermediate results as view-consistency features for the only variation is whether cross-attention incorporated or not. In this case, during each denoising step, we apply scaled-up consistency features as gradient guidance, enabling diffusion to adjust the generation direction toward consistent results.

Since the reference image’s texture is unknown for unseen views, relying solely on coarse text descriptions can cause inconsistencies. To address this, we propose prompt-tuning-based gradient guidance to encode texture characteristics differences into additional prompt tokens. Specifically, we align the token with the difference between the reference and unedited images in the CLIP feature space [8], capturing the texture transformation direction. This difference guides the diffusion denoising process, ensuring consistent texture transfer across views. Applying this finetuned prompt as gradient guidance significantly improves texture style consistency in unseen views while preserving details in reference views.

We evaluate our method on face-forwarding [30] and 360-degree [3] datasets with diverse 3D swapping edits. Results show that our approach effectively transfers textures while preserving fine details and ensuring superior view consistency. Our key contributions are:

- *3DSwapping*, a novel 3D swapping method enabling efficient and flexible 3D editing from a reference 2D image.
- The progressive generation process with view-consistency gradient guidance to mitigate view inconsistency problem.
- Prompt-tuning-based gradient guidance to preserve texture characteristics difference in seen views and ensure style consistency in unseen views.
- Extensive experiments demonstrating that *3DSwapping* achieves SOTA visual and numerical performance.

2. Related Work

2D Diffusion-based Editing DragDiffusion [26] utilizes key points to define target images and edit source images, achieving swapping by replacing key point-based targets with reference images. A-Tale-of-Two-Features [37] exploits the dense semantic correspondence of DINO [5] and the sparse spatial awareness of diffusion features to perform texture swapping by merging DINO features from the reference view with diffusion features from the target view. Plug-and-Play [28] refines high-frequency, fine-grained details by injecting diffusion features into DINO features, following A-Tale-of-Two-Features to enable image swapping. DiffEditor [20] enhances 2D editing flexibility and precision by integrating stochastic differential equations into ordinary differential equation sampling while incorporating

regional gradient guidance and a time-travel strategy. The most relevant work, SwapAnything [10], employs DreamBooth [24] to encode source image into a specialized token and utilizes AdaIN [16] to maintain style consistency in swapped region, enabling direct 2D image swapping. While these methods achieve 2D swapping with minor modifications, they process images independently, lacking view consistency. This limitation underscores the need for a swapping technique tailored for 3D applications.

3D Editing 3D editing methods leverage the capabilities of 2D editing models (e.g., diffusion) as guidance and adopt dataset-updating strategies to finetune pretrained 3D scenes. Instruct-NeRF2NeRF [13] and Instruct-GS2GS [29] utilize instruct-pix2pix [4] for 2D image guidance, updating 3D datasets for subsequent NeRF or Gaussian splatting finetuning. GaussianEditor [7] enhances the Gaussian splatting pipeline with hierarchical representations, ensuring stable editing performance under stochastic generative model guidance. Direct Gaussian Editor (DGE) [6] addresses view consistency using an epipolar cross-attention mechanism. It first generates edited images independently based on a text prompt, then applies epipolar cross-attention between these edits and the remaining unedited images. However, the initial independent generation step introduces inconsistencies, leading to undesired artifacts. GaussCtrl [34] tackles view inconsistency by injecting features from unedited reference views to maintain geometry and texture consistency. However, relying on unedited images presents challenges—when editing individual images, the diffusion model also retains texture information from the original dataset, causing generated images to resemble unedited ones. This limitation constrains the applicability of edits to cases with similar textures.

Methods [7, 13, 29] that disregard view consistency can be adapted for 3D swapping by integrating image captioning techniques. For consistency-aware approaches [6, 34], a straightforward solution is to project reference images into latent space and use them as initialization in the denoising process. This propagates the desired texture across multiple views, enabling fine-tuning of pretrained 3D scenes for improved coherence and realism. However, these naive modifications offer only basic functionality; achieving visually compelling swaps that preserve object identity demands more precise adaptations.

3. Proposed Method

Fig. 2 shows our *3DSwapping* pipeline, which comprises three key modules: 1) a progressive generation process, 2) view-consistency gradient guidance for maintaining coherence, and 3) prompt-tuning-based gradient guidance for preserving object characteristics.

First, we generate multiple candidate images conditioned

on depth information, allowing the user to select the one best aligned with the desired attributes as the reference image. Next, following [34], we encode both the reference and unedited images into latent space as the starting point for the denoising process. We then apply prompt-tuning to extract texture characteristic differences between references and 3D objects, and further guide diffusion denoising process, ensuring object identity preservation. Finally, we progressively edit the original training set, starting from the reference view. The updated dataset is then used to iteratively finetune the 3D Gaussian model.

3.1. Progressive Generation

As discussed in the previous section, existing methods [6, 7, 13, 29, 34] struggle with view consistency and editing flexibility. For instance, GaussCtrl [34] conditions diffusion inference on unedited images, preserving consistency at the cost of editing flexibility, often causing objects to retain their original texture. DGE [6] reduces dependence on unedited images but introduces a non-adjacent view editing step, leading to inconsistencies. To address these limitations, we propose a progressive generation process that eliminates reliance on unedited images and avoids independent generation steps, ensuring both consistency and flexibility.

To generate reference images, we condition the generative model on depth information with the background masked out, ensuring geometric alignment. However, the generated images often fail to precisely match the target geometry. To mitigate this, we refine the depth using masks processed with dilation and blurring. We apply the original unprocessed mask to the generated candidates to eliminate redundant content.

For the selected reference view τ and the i -th image $\mathbb{I}i$ to be swapped, we construct a sparse reference set $\mathbb{R}i = \mathbb{I}\tau, \mathbb{I}i - 1, \mathbb{F}(\mathbb{I})\tau$ without background. The inclusion of $\mathbb{I}i - 1$ ensures minimal angle change, preserving local view consistency. As editing progresses to more distant views, errors accumulate from previous generations, and using non-adjacent views introduces inconsistencies. To mitigate this, we incorporate $\mathbb{I}\tau$ along with its horizontally flipped counterpart $\mathbb{F}(\mathbb{I})\tau$ in the reference set. This maintains efficiency by reducing the number of required conditioning images while ensuring faithful swapping.

We condition the generative model on the reference set \mathbb{R} using weighted fused cross-attention to generate edited images:

$$\text{WeightedAttn}_e = \lambda \text{Attn}_{e,e} + (1 - \lambda) \sum_{i \in \mathbb{R}} w_i \text{Attn}_{e,i}, \quad (1)$$

where $\text{Attn}_{i,j}$ represents the attention score between images i and j . The partial denoising process is first applied to the reference view, then expanded to adjacent views. Af-

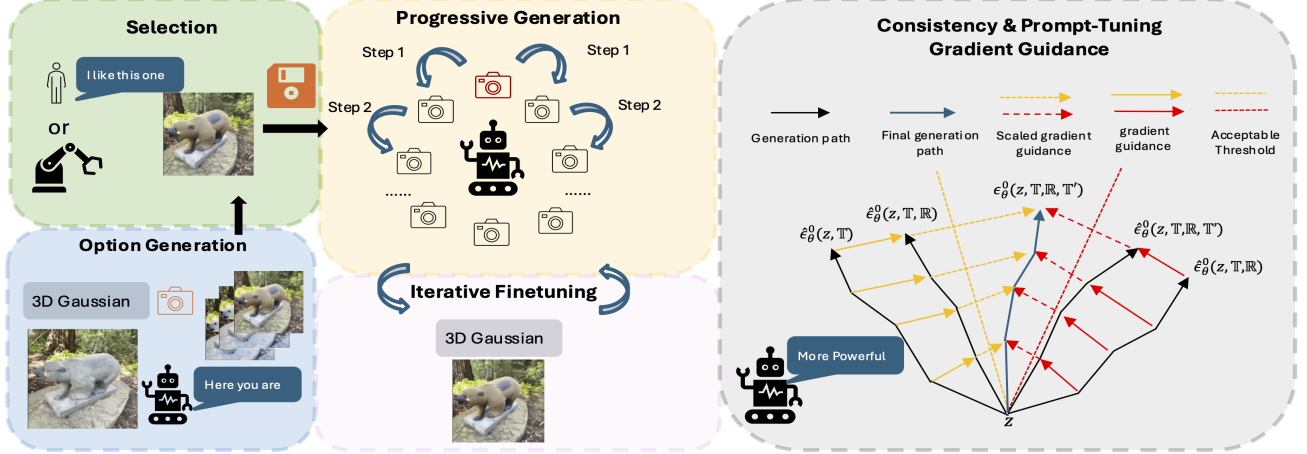


Figure 2. **3DSwapping**. Our framework enables 3D swapping by generating multiple reference image options for user selection. During editing, we employ a progressive generation process enhanced by view-consistency gradient guidance and prompt-tuning-based gradient guidance to preserve both consistency and identity. Here, \mathbb{R} , \mathbb{T} , and \mathbb{T}' refer to the reference set, text prompt and finetuned prompt, respectively.

ter the editing process, we use those edited view-consistent images to finetune 3D gaussians and conduct the above procedure iteratively.

3.2. View-Consistency Gradient Guidance

Existing generative models [9, 24, 36, 38] rely on numerous reference views to maintain view consistency, whereas our progressive generation approach begins with a single reference and uses only a few views for editing. To ensure consistency under this limited-reference setting, we introduce a consistency-aware gradient guidance mechanism that enhances the backbone’s ability to enforce view consistency throughout the generation process.

Given the image $\mathbb{I}i$ to be edited, the reference set is defined as $\mathbb{R}i = \mathbb{I}\tau, \mathbb{I}i - 1, \mathbb{F}(\mathbb{I})_\tau$, as described in 3.1. The denoising process is formulated as:

$$\begin{aligned} \epsilon_\theta^t(z_\lambda, \mathbb{T}, \mathbb{R}) &= \epsilon_{\hat{\theta}}^t(z_\lambda) \\ &+ w_{\mathbb{T}}(\epsilon_{\hat{\theta}}^t(z_\lambda, \mathbb{T}, \mathbb{R}) - \epsilon_{\hat{\theta}}^t(z_\lambda, \mathbb{R})) \\ &+ w_{\mathbb{R}}(\epsilon_{\hat{\theta}}^t(z_\lambda, \mathbb{T}, \mathbb{R}) - \epsilon_{\hat{\theta}}^t(z_\lambda, \mathbb{T})), \end{aligned} \quad (2)$$

where \mathbb{T} refers to the text prompt condition, θ and $\hat{\theta}$ refer to diffusion with and without weighted fused cross-attention, $w_{\mathbb{T}}$ and $w_{\mathbb{R}}$ refer to scaling factor for each term. The partial denoising process can then be expressed as:

$$\begin{aligned} z^{(t-1|\kappa)} &= \sqrt{\alpha_{t-1|\kappa}} \frac{z^{t|\kappa} - \sqrt{1 - \alpha_{t|\kappa}} \cdot \epsilon_\theta^{t|\kappa}(z, \mathbb{T}, \mathbb{R})}{\sqrt{\alpha_{t|\kappa}}} \\ &+ \sqrt{1 - \alpha_{t-1|\kappa}} \epsilon_\theta^{t|\kappa}(z, \mathbb{T}, \mathbb{R}), \end{aligned} \quad (3)$$

where step $t \in [0, \kappa]$, $\kappa_\tau < \kappa_{i \neq \tau}$, α refers to the scheduling coefficient in DDIM scheduler, and $z^{(t-1|\kappa)}$ refers to the

latent feature obtained by Eq.(4) and conducted till κ -th step:

$$z^{t+1} = \sqrt{\alpha_{t+1}} \frac{z^t - \sqrt{1 - \alpha_t} \cdot \epsilon^t}{\sqrt{\alpha_t}} + \sqrt{1 - \alpha_{t+1}} \epsilon^t. \quad (4)$$

The second term $w_{\mathbb{T}}(\epsilon_\theta^t(z_\lambda, \mathbb{T}, \mathbb{R}) - \epsilon_\theta^t(z_\lambda, \mathbb{R}))$ in Eq.(2) extracts difference between results generated with and without negative text prompt [14], which improves the fidelity of the editing prompt to text prompt. The third term $w_{\mathbb{R}}(\epsilon_\theta^t(z_\lambda, \mathbb{T}, \mathbb{R}) - \epsilon_\theta^t(z_\lambda, \mathbb{T}))$ improves the view consistency. Intuitively, the third term captures variations in generations induced by reference set conditions. Amplifying this difference enables the generative model to refine its generation path, ensuring texture consistency. This process enhances the backbone without requiring additional training cost.

3.3. Prompt-tuning-based Gradient Guidance

Text descriptions provide coarse-grained control during the diffusion process, often leading to a loss of object identity and texture fidelity. For instance, the term ”stone bear” could refer to bears made of different-colored stones with varying shapes. Among diffusion fine-tuning methods [9, 15, 24, 36], textual inversion [9] optimizes a special token embedding for texture or object specific description. However, it still requires multiple images to achieve satisfactory quality (please refer to supplementary material for results using a single image). To address this, we propose prompt-tuning-based gradient guidance, reducing the need for multi training images while effectively encoding texture characteristics. The core idea is to use prompt-tuning to learn a new token that encodes the texture differences between the unedited 3D object and the reference image. This

token emphasizes texture differences during the denoising process, guiding the reconstruction toward the reference texture style.

Given the reference image \mathbb{I}_τ and its corresponding unedited rendered image $\hat{\mathbb{I}}_\tau$ in CLIP feature space, we compute the texture difference $\Delta_{\hat{\mathbb{I}}_\tau \rightarrow \mathbb{I}_\tau}$ as:

$$\Delta_{\hat{\mathbb{I}}_\tau \rightarrow \mathbb{I}_\tau} = \text{Clip}(\hat{\mathbb{I}}_\tau) - \text{Clip}(\mathbb{I}_\tau). \quad (5)$$

This texture difference serves as the ground truth when generating \mathbb{I}_τ from $\hat{\mathbb{I}}_\tau$ and further guides the generation direction in the diffusion process.

We randomly initialize the text prompt $\hat{\mathbb{T}}$, which has been shown to outperform initialization with the original text prompt in [21]. The prompt is first optimized using the texture difference $\Delta_{\hat{\mathbb{I}}_\tau \rightarrow \mathbb{I}_\tau}$ in CLIP space, defined as:

$$L_{\text{clip}} = \text{cosine}(\Delta_{\hat{\mathbb{I}}_\tau \rightarrow \mathbb{I}_\tau} \rightarrow \mathbb{I}_\tau, \hat{\mathbb{T}}). \quad (6)$$

To further bridge the gap between image and text features in CLIP space, we perform additional prompt tuning in diffusion feature space using:

$$L_{\text{diff}} = \epsilon\theta(z_\lambda, \mathbb{T}', \mathbb{R}) - \epsilon'\theta(z_\lambda, \mathbb{T}', \mathbb{R}). \quad (7)$$

This ensures a more effective alignment between text and visual features, enhancing consistency in the generation process.

Although the auxiliary text prompt \mathbb{T}' captures texture differences, it exhibits oscillations during training and struggles to precisely describe texture characteristics. Moreover, the direction of texture style changes is not inherently meaningful in text form compared to directly encoding style features. As a result, relying solely on the learned prompt fails to achieve fine-grained control. To address this, we integrate the auxiliary text prompt into the denoising process as gradient guidance. The denoising Eq.(2) is thus reformulated as:

$$\begin{aligned} \epsilon_\theta^t(z_\lambda, \mathbb{T}, \mathbb{R}, \mathbb{T}') &= \epsilon_\theta^t(z_\lambda) \\ &+ w_{\mathbb{T}}(\epsilon_\theta^t(z_\lambda, \mathbb{T}, \mathbb{R}) - \epsilon_\theta^t(z_\lambda, \mathbb{R})) \\ &+ w_{\mathbb{R}}(\epsilon_\theta^t(z_\lambda, \mathbb{T}, \mathbb{R}) - \epsilon_\theta^t(z_\lambda, \mathbb{T})) \\ &+ w_{\mathbb{T}'}(\epsilon_\theta^t(z_\lambda, \mathbb{T}', \mathbb{R}) - \epsilon_\theta^t(z_\lambda, \mathbb{T}, \mathbb{R})). \end{aligned} \quad (8)$$

4. Experiments

We compare our method with state-of-the-art text-driven editing approaches, including GaussCtrl [34], DGE [6], IGS2GS [29], and IN2N [13]. Since these methods rely on text inputs, we use captioned descriptions as editing prompts to enable swapping functionality. For quantitative evaluation, we employ AlexNet-based [19] and VGG-based [27] LPIPS scores [39], CLIP score [23], and Vision-GPT score [1], supplemented by user studies. Comparisons

are conducted across multiple scenes from different datasets to ensure a comprehensive assessment following [34].

4.1. Quantitative Evaluation

For each edit, we compute AlexNet-based and VGG-based LPIPS scores, CLIP score, Vision-GPT score, and conduct user studies, as summarized in Table 1. Detailed per-scene scores are provided in the supplementary material. LPIPS and CLIP scores serve as perceptual evaluation metrics, measuring feature similarity. LPIPS ranges from 0 to 1, with lower values indicating better perceptual quality, while higher CLIP scores are preferred. Vision-GPT assesses the faithfulness of swapped textures from the reasoning perspective, scoring from 0 to 100, where higher values indicate better alignment. For user studies, participants are informed of the edited object and required to rate the 3D result on a scale of 1 to 5, with higher scores reflecting better quality. Quantitative results show that our method achieves the highest performance across all metrics.

Edits	IN2N	IGS2GS	GaussCtrl	DGE	Ours
CLIP Score \uparrow	0.8917	0.8908	0.8638	0.8572	0.9333
Lpips(Alex) \downarrow	0.1708	0.1683	0.1692	0.1713	0.1166
Lpips(VGG) \downarrow	0.1676	0.1594	0.1591	0.1603	0.1247
Vision-GPT \uparrow	45.5	52	48	54	76
User study \uparrow	2.0600	2.5600	2.1200	2.1200	4.5400

Table 1. Quantitative results evaluated by CLIP score, VGG-based and Alex-based LPIPS scores, Vision-GPT and user studies given reference image with rendered edited objects. **Bold** text refers to the best performance and underlined text refers to the second best performance. Detailed results can be found in Supp.

4.2. Qualitative Evaluation

We present qualitative results of 360-degree dataset in Figs.1, Figs.3 and 4. Fig.3 and 3 includes reference images with texture color or material variations, while Fig.4 features those with complex textures and significant semantic changes. Fig.5 shows the results of "face-forward" case.

Our method, with its swapping capability, enables more precise 3D object editing without unintended texture leakage between objects. In the 360-degree color and material editing scenario (e.g., bear and table), IN2N [13] and IGS2GS [29] suffer from incorrect color saturation and inaccurate material representation. In the bear scenarios (Fig.1, 3a), their results are under-saturated, whereas in the table scenarios (Fig.3b, 1), they are over-saturated. None of the baseline methods accurately reproduce the intended material attributes (i.e., plastic, moss in Fig. 1 and metallic in Fig. 3a). GaussCtrl [34] excessively preserves the original 3D object’s appearance, resulting in minimal modifications due to its unedited reference set. Our method effectively swaps textures while achieving realistic material ap-

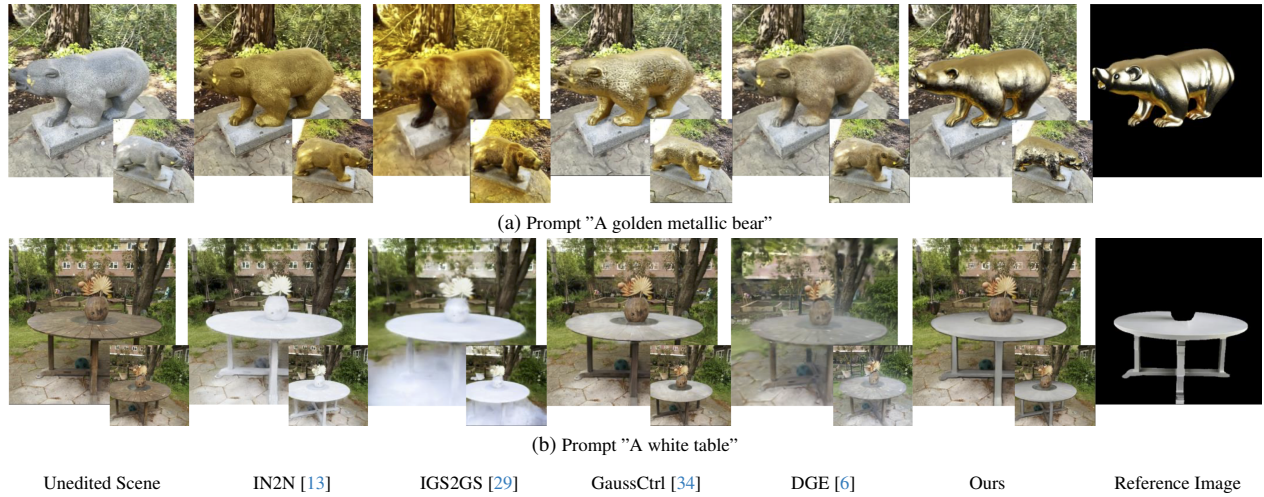


Figure 3. Qualitative comparison on 360-degree scenes (material and color edits): Our 3DSwapping method faithfully swaps texture from reference images to 3D objects. Our method edits 3D objects faithfully to reference images' texture and geometry.

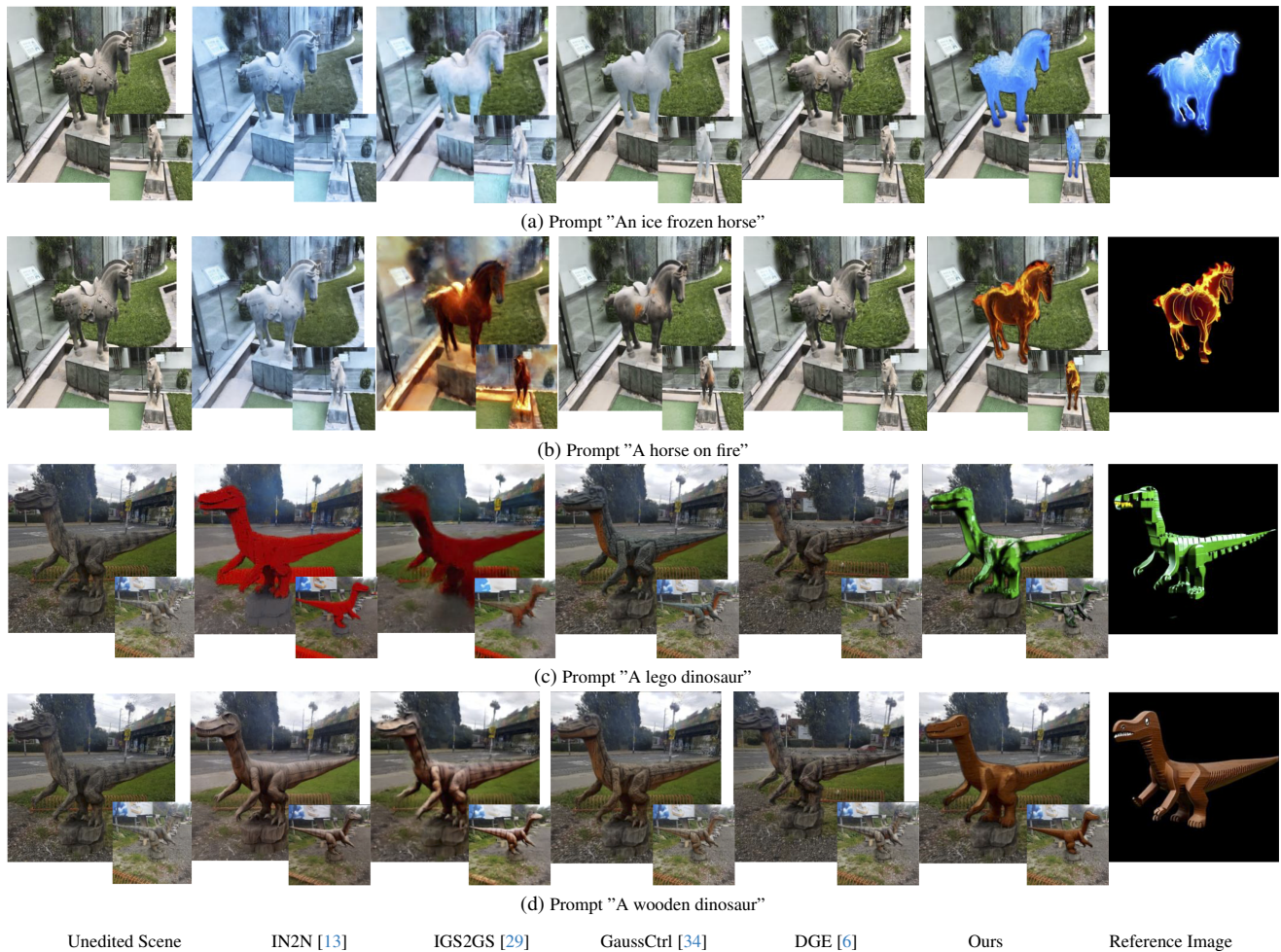


Figure 4. Qualitative comparison on 360-degree scenes (complicated texture edits): Our 3DSwapping method successfully swaps complicated texture from reference images to 3D objects.



Figure 5. Qualitative comparison on face-forwarding scenes: Our 3Dswapping method faithfully swaps texture from reference images to 3D objects and generates the most plausible texture edits for unseen view.

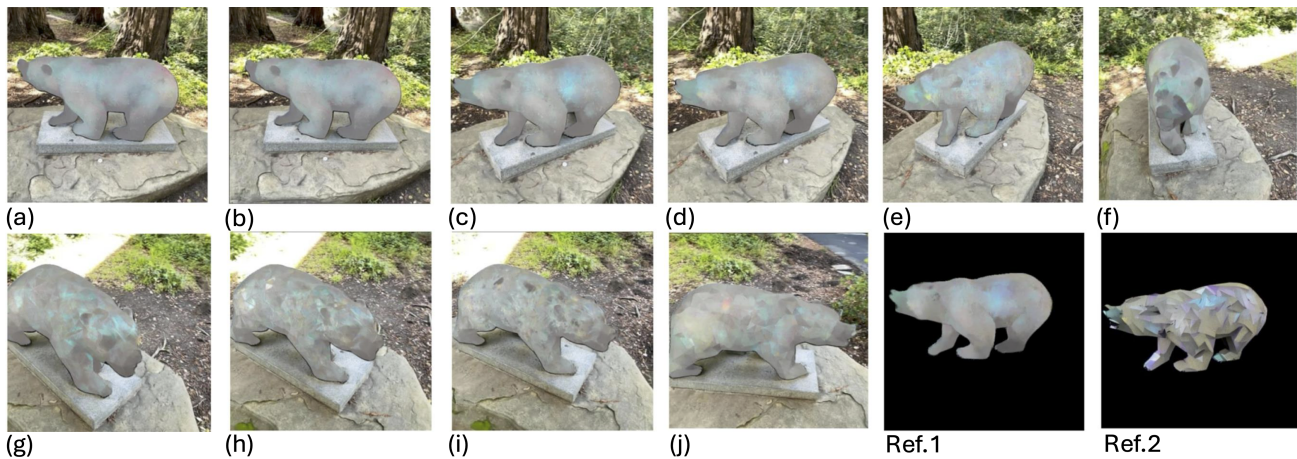


Figure 6. Ablation study on prompt-tuning-based gradient guidance: The editing prompt is "A colorful metal bear." Views (a)–(d) overlap with the reference view Ref.1 and closely match its characteristics. In contrast, the unseen views (e)–(j) resemble Ref.2, which was used for prompt-tuning, effectively preserving its characteristic details.

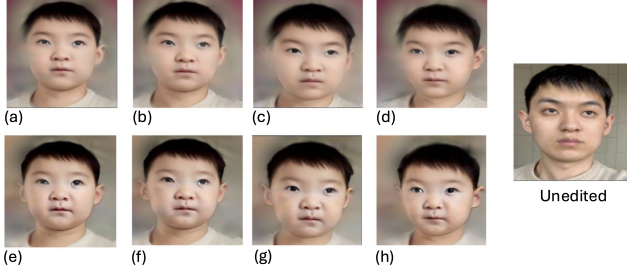


Figure 7. Ablation study on view-consistency gradient guidance: The editing prompt is "A baby face." Figures (a) - (d) show 3D objects edited without view-consistency gradient guidance; figures (e) - (h) are results with guidance of view-consistency gradient.

pearances, such as specular highlights on the bear and the lush, velvety moss on the table. In *moss-covered table* scenario (Fig.1), all the 3D baseline methods only attempt to swap texture while ours can also modify geometry to better match the "moss material".

In the large semantic change swapping scenario (Fig.4), baseline methods struggle with significant transformations. DGE [6] often fails, as its edits remain nearly unchanged. Its initial independent editing stage leading to inconsistent results, and further causing the epipolar attention mechanism to break down in highly dissimilar views, resulting in minimal overall changes. Our method achieves precise 3D object editing with a texture style that closely matches the reference image, enabled by our proposed prompt-tuning, consistency guidance, and progressive process. Prompt-tuning preserves intricate texture details, while consistency guidance and progressive generation mitigate blurriness from view inconsistency.

In the face-forward case (Fig.5), our method preserves fine details, such as the black lower eyelid and feather-like cloth in the hawk scenario (Fig.5a). IN2N [13] and IGS2GS [29] generate erroneous results due to their independent diffusion process and full diffusion steps. The independent generation process leads to inconsistent images, while full diffusion steps cause excessive texture changes and identity loss. Finetuning NeRF with these inconsistent and identity-lost images can result in network collapse. For GaussCtrl [34] and DGE [6], particularly in the hawk case, large texture differences break their view-consistency mechanisms, resulting in outputs that retain the original object's appearance instead of the intended modifications.

4.3. Ablation Studies

Prompt-tuning based Gradient Guidance We highlight the effectiveness of prompt-tuning-based gradient guidance by using a prompt embedding trained on reference image Ref-2 to edit reference image Ref-1, as shown in Fig. 6. Ref-2 depicts a bear with sharp metallic edges, while Ref-1 features a rusted metal appearance. In Fig. 6, subfig-

ures (a)–(d) correspond to the overlapping region with Ref-1, producing rendered results that closely resemble Ref-1. However, for the unseen side (subfigures (e)–(j)), where the texture is undefined, the learned prompt embedding plays a crucial role in guiding the generation toward the "colorful metal bear" appearance. This ensures that the output aligns more closely with Ref-2, demonstrating the effectiveness of our prompt-tuning-based gradient guidance in learning specific textures and steering the generation process.

View-consistency Gradient Guidance We demonstrate the importance of view-consistency gradient guidance by comparing rendered images of objects edited with a view-consistency scaling factor $w_{\mathbb{R}}$ of 0 (i.e., no guidance) and 1. Subfigures (a) - (d) in Fig.7 show renders with a scaling factor of $w_{\mathbb{R}} = 0$, while subfigures e-h use $w_{\mathbb{R}} = 1$. The blurry reconstructed regions indicate areas of inconsistency [6]. The left cheeks in subfigures (a) - (d) exhibit severe blurriness, whereas our approach achieves significantly improved consistency. This demonstrates the effectiveness of our view-consistency gradient guidance.

4.4. Discussion

Our method ensures that reference images maintain similar geometry by leveraging a depth-conditioned generative model. Using a reference object with a different shape is incompatible with our reference set construction process and may introduce artifacts if directly used as a reference image. Our approach also allows 3D Gaussian geometry updates to better align with reference images, but a mismatched shape in the reference image could destabilize this process, leading to the collapse of 3D Gaussians. A possible workaround is to apply 2D swapping techniques [11, 12, 17, 22, 26, 31, 33, 35, 36] to transfer differently shaped reference images onto an unedited view before incorporating them into our 3D swapping pipeline. However, this primarily pertains to 2D editing and falls outside the scope of our current work.

The quality of unedited 3D Gaussians also impacts editing performance. Undertrained Gaussian spheres (e.g., floating Gaussians in empty space) degrade rendered images, disrupting the mask generation process. Incorrect segmentation can result in edits with significantly altered geometry, ultimately causing 3D Gaussian collapse.

5. Conclusion

We introduced 3DSwapping, enabling 3D object texture swapping from reference images, a new capability in the 3D editing field. To achieve this, we proposed three key techniques: (1) progressive generation, (2) view-consistency gradient guidance, and (3) prompt-tuning-based guidance. These components effectively address challenges related to

view consistency and texture preservation during 3D swapping. We evaluated our method on multiple scenes across color, material, and large semantic change swapping scenarios. Our approach outperforms all baselines significantly.

References

- [1] Josh Achiam, Steven Adler, Sandhini Agarwal, Lama Ahmad, Ilge Akkaya, Florencia Leoni Aleman, Diogo Almeida, Janko Altenschmidt, Sam Altman, Shyamal Anadkat, et al. Gpt-4 technical report. *arXiv preprint arXiv:2303.08774*, 2023. 5
- [2] Shivangi Aneja, Justus Thies, Angela Dai, and Matthias Nießner. Clipface: Text-guided editing of textured 3d malleable models. In *ACM SIGGRAPH 2023 Conference Proceedings*, pages 1–11, 2023. 2
- [3] Jonathan T Barron, Ben Mildenhall, Dor Verbin, Pratul P Srinivasan, and Peter Hedman. Mip-nerf 360: Unbounded anti-aliased neural radiance fields. In *Proceedings of the IEEE/CVF conference on computer vision and pattern recognition*, pages 5470–5479, 2022. 2
- [4] Tim Brooks, Aleksander Holynski, and Alexei A Efros. Instructpix2pix: Learning to follow image editing instructions. In *Proceedings of the IEEE/CVF Conference on Computer Vision and Pattern Recognition*, pages 18392–18402, 2023. 3
- [5] Mathilde Caron, Hugo Touvron, Ishan Misra, Hervé Jégou, Julien Mairal, Piotr Bojanowski, and Armand Joulin. Emerging properties in self-supervised vision transformers. In *Proceedings of the IEEE/CVF international conference on computer vision*, pages 9650–9660, 2021. 2
- [6] Minghao Chen, Iro Laina, and Andrea Vedaldi. Dge: Direct gaussian 3d editing by consistent multi-view editing. *arXiv preprint arXiv:2404.18929*, 2024. 2, 3, 5, 6, 7, 8
- [7] Yiwen Chen, Zilong Chen, Chi Zhang, Feng Wang, Xiaofeng Yang, Yikai Wang, Zhongang Cai, Lei Yang, Huaping Liu, and Guosheng Lin. Gaussianeditor: Swift and controllable 3d editing with gaussian splatting. In *Proceedings of the IEEE/CVF Conference on Computer Vision and Pattern Recognition*, pages 21476–21485, 2024. 2, 3
- [8] Mehdi Cherti, Romain Beaumont, Ross Wightman, Mitchell Wortsman, Gabriel Ilharco, Cade Gordon, Christoph Schuhmann, Ludwig Schmidt, and Jenia Jitsev. Reproducible scaling laws for contrastive language-image learning. In *Proceedings of the IEEE/CVF Conference on Computer Vision and Pattern Recognition*, pages 2818–2829, 2023. 2
- [9] Rinon Gal, Yuval Alaluf, Yuval Atzmon, Or Patashnik, Amit H Bermano, Gal Chechik, and Daniel Cohen-Or. An image is worth one word: Personalizing text-to-image generation using textual inversion. *arXiv preprint arXiv:2208.01618*, 2022. 2, 4
- [10] Jing Gu, Yilin Wang, Nanxuan Zhao, Wei Xiong, Qing Liu, Zhifei Zhang, He Zhang, Jianming Zhang, HyunJoon Jung, and Xin Eric Wang. Swapananything: Enabling arbitrary object swapping in personalized visual editing. *arXiv preprint arXiv:2404.05717*, 2024. 2, 3
- [11] Yuchao Gu, Yipin Zhou, Bichen Wu, Licheng Yu, Jia-Wei Liu, Rui Zhao, Jay Zhangjie Wu, David Junhao Zhang, Mike Zheng Shou, and Kevin Tang. Videoswap: Customized video subject swapping with interactive semantic point correspondence. In *Proceedings of the IEEE/CVF Conference on Computer Vision and Pattern Recognition*, pages 7621–7630, 2024. 8
- [12] Yue Han, Junwei Zhu, Keke He, Xu Chen, Yanhao Ge, Wei Li, Xiangtai Li, Jiangning Zhang, Chengjie Wang, and Yong Liu. Face-adapter for pre-trained diffusion models with fine-grained id and attribute control. In *European Conference on Computer Vision*, pages 20–36. Springer, 2024. 8
- [13] Ayaan Haque, Matthew Tancik, Alexei A Efros, Aleksander Holynski, and Angjoo Kanazawa. Instruct-nerf2nerf: Editing 3d scenes with instructions. In *Proceedings of the IEEE/CVF International Conference on Computer Vision*, pages 19740–19750, 2023. 2, 3, 5, 6, 7, 8
- [14] Jonathan Ho and Tim Salimans. Classifier-free diffusion guidance. *arXiv preprint arXiv:2207.12598*, 2022. 4
- [15] Edward J Hu, Yelong Shen, Phillip Wallis, Zeyuan Allen-Zhu, Yuanzhi Li, Shean Wang, Lu Wang, and Weizhu Chen. Lora: Low-rank adaptation of large language models. *arXiv preprint arXiv:2106.09685*, 2021. 4
- [16] Xun Huang and Serge Belongie. Arbitrary style transfer in real-time with adaptive instance normalization. In *Proceedings of the IEEE international conference on computer vision*, pages 1501–1510, 2017. 3
- [17] Yuming Jiang, Tianxing Wu, Shuai Yang, Chenyang Si, Dahua Lin, Yu Qiao, Chen Change Loy, and Ziwei Liu. Videobooth: Diffusion-based video generation with image prompts. In *Proceedings of the IEEE/CVF Conference on Computer Vision and Pattern Recognition*, pages 6689–6700, 2024. 8
- [18] Umar Khalid, Hasan Iqbal, Azib Farooq, Jing Hua, and Chen Chen. 3dego: 3d editing on the go! In *European Conference on Computer Vision*, pages 73–89. Springer, 2024. 2
- [19] Alex Krizhevsky, Ilya Sutskever, and Geoffrey E Hinton. Imagenet classification with deep convolutional neural networks. *Advances in neural information processing systems*, 25, 2012. 5
- [20] Chong Mou, Xintao Wang, Jiechong Song, Ying Shan, and Jian Zhang. Diffeditor: Boosting accuracy and flexibility on diffusion-based image editing. In *Proceedings of the IEEE/CVF Conference on Computer Vision and Pattern Recognition*, pages 8488–8497, 2024. 2
- [21] Thao Nguyen, Yuheng Li, Utkarsh Ojha, and Yong Jae Lee. Visual instruction inversion: Image editing via image prompting. *Advances in Neural Information Processing Systems*, 36, 2024. 5
- [22] Xingang Pan, Ayush Tewari, Thomas Leimkühler, Lingjie Liu, Abhimitra Meka, and Christian Theobalt. Drag your gan: Interactive point-based manipulation on the generative image manifold. In *ACM SIGGRAPH 2023 conference proceedings*, pages 1–11, 2023. 8
- [23] Alec Radford, Jong Wook Kim, Chris Hallacy, Aditya Ramesh, Gabriel Goh, Sandhini Agarwal, Girish Sastry, Amanda Askell, Pamela Mishkin, Jack Clark, et al. Learning transferable visual models from natural language supervision. In *International conference on machine learning*, pages 8748–8763. PMLR, 2021. 5

- [24] Nataniel Ruiz, Yuanzhen Li, Varun Jampani, Yael Pritch, Michael Rubinstein, and Kfir Aberman. Dreambooth: Fine tuning text-to-image diffusion models for subject-driven generation. In *Proceedings of the IEEE/CVF conference on computer vision and pattern recognition*, pages 22500–22510, 2023. 2, 3, 4
- [25] Taha Samavati and Mohsen Soryani. Deep learning-based 3d reconstruction: a survey. *Artificial Intelligence Review*, 56(9):9175–9219, 2023. 2
- [26] Yujun Shi, Chuhui Xue, Jun Hao Liew, Jiachun Pan, Han-shu Yan, Wenqing Zhang, Vincent YF Tan, and Song Bai. Dragdiffusion: Harnessing diffusion models for interactive point-based image editing. In *Proceedings of the IEEE/CVF Conference on Computer Vision and Pattern Recognition*, pages 8839–8849, 2024. 2, 8
- [27] Karen Simonyan and Andrew Zisserman. Very deep convolutional networks for large-scale image recognition. *arXiv preprint arXiv:1409.1556*, 2014. 5
- [28] Narek Tumanyan, Michal Geyer, Shai Bagon, and Tali Dekel. Plug-and-play diffusion features for text-driven image-to-image translation. In *Proceedings of the IEEE/CVF Conference on Computer Vision and Pattern Recognition*, pages 1921–1930, 2023. 1, 2
- [29] Cyrus Vachha and Ayaan Haque. Instruct-gs2gs: Editing 3d gaussian splats with instructions, 2024. 1, 2, 3, 5, 6, 7, 8
- [30] Can Wang, Ruixiang Jiang, Menglei Chai, Mingming He, Dongdong Chen, and Jing Liao. Nerf-art: Text-driven neural radiance fields stylization. *IEEE Transactions on Visualization and Computer Graphics*, 2023. 2
- [31] Peng Wang and Yichun Shi. Imagedream: Image-prompt multi-view diffusion for 3d generation. *arXiv preprint arXiv:2312.02201*, 2023. 8
- [32] Yuxuan Wang, Xuanyu Yi, Zike Wu, Na Zhao, Long Chen, and Hanwang Zhang. View-consistent 3d editing with gaussian splatting. In *European Conference on Computer Vision*, pages 404–420. Springer, 2024. 2
- [33] Yujie Wei, Shiwei Zhang, Zhiwu Qing, Hangjie Yuan, Zhiheng Liu, Yu Liu, Yingya Zhang, Jingren Zhou, and Hongming Shan. Dreamvideo: Composing your dream videos with customized subject and motion. In *Proceedings of the IEEE/CVF Conference on Computer Vision and Pattern Recognition*, pages 6537–6549, 2024. 8
- [34] Jing Wu, Jia-Wang Bian, Xinghui Li, Guangrun Wang, Ian Reid, Philip Torr, and Victor Adrian Prisacariu. Gaussctrl: multi-view consistent text-driven 3d gaussian splatting editing. *arXiv preprint arXiv:2403.08733*, 2024. 1, 2, 3, 5, 6, 7, 8
- [35] Yihang Wu, Xiao Cao, Kaixin Li, Zitan Chen, Haonan Wang, Lei Meng, and Zhiyong Huang. Towards better text-to-image generation alignment via attention modulation. *arXiv preprint arXiv:2404.13899*, 2024. 8
- [36] Hu Ye, Jun Zhang, Sibao Liu, Xiao Han, and Wei Yang. Ip-adapter: Text compatible image prompt adapter for text-to-image diffusion models. *arXiv preprint arXiv:2308.06721*, 2023. 4, 8
- [37] Junyi Zhang, Charles Herrmann, Junhwa Hur, Luisa Polania Cabrera, Varun Jampani, Deqing Sun, and Ming-Hsuan Yang. A tale of two features: Stable diffusion complements dino for zero-shot semantic correspondence. *Advances in Neural Information Processing Systems*, 36, 2024. 2
- [38] Lvmin Zhang, Anyi Rao, and Maneesh Agrawala. Adding conditional control to text-to-image diffusion models. In *Proceedings of the IEEE/CVF International Conference on Computer Vision*, pages 3836–3847, 2023. 2, 4
- [39] Richard Zhang, Phillip Isola, Alexei A Efros, Eli Shechtman, and Oliver Wang. The unreasonable effectiveness of deep features as a perceptual metric. In *Proceedings of the IEEE conference on computer vision and pattern recognition*, pages 586–595, 2018. 5
- [40] Chenyang Zhu, Kai Li, Yue Ma, Longxiang Tang, Chengyu Fang, Chubin Chen, Qifeng Chen, and Xiu Li. Instantswap: Fast customized concept swapping across sharp shape differences. *arXiv preprint arXiv:2412.01197*, 2024. 2
- [41] Jingyu Zhuang, Chen Wang, Liang Lin, Lingjie Liu, and Guanbin Li. Dreameditor: Text-driven 3d scene editing with neural fields. In *SIGGRAPH Asia 2023 Conference Papers*, pages 1–10, 2023. 2